

## Pressure-Raman effects and vibrational scaling laws in molecular crystals: $S_8$ and $As_2S_3$

Richard Zallen

Xerox Research Laboratories, Rochester, New York 14580\*  
 Department of Physics, Technion-Israel Institute of Technology, Haifa, Israel  
 (Received 19 December 1973)

The influence of pressure on lattice vibrations in two molecular crystals, the ring-molecule elemental crystal orthorhombic sulfur and the layer-structure chalcogenide crystal  $As_2S_3$ , has been measured by observations of their first-order Raman-scattering spectra at pressures to 10 kbar. Experimental results on the many Raman-active modes in each of these crystals reveal that, in contrast to network crystals, the compression-induced shifts of the optical-phonon frequencies in molecular crystals are strikingly *inconsistent* with the usual frequency-volume Grüneisen scaling law. Far from being frequency independent, the mode-Grüneisen parameter  $\gamma_i = (\Delta\bar{\nu}_i/\bar{\nu}_i) (-\Delta V/V)^{-1}$  varies strongly and *systematically* with mode frequency  $\bar{\nu}_i$  over the optical-phonon spectrum, falling sharply from values of order 1 at low frequencies to values of order  $10^{-2}$  at high frequencies.  $\gamma_i$  is thus of "normal" size for external modes but is "anomalously" small for internal modes. Although we must abandon  $\bar{\nu}_i \sim V^{-\gamma}$  (with  $\gamma$  independent of  $i$ ) for molecular crystals, the idea of a basic vibrational scaling law can be preserved in the form of the *bond-stiffness-bond-length* relation  $k \sim r^{-6\gamma}$ . Here  $k$  is the force constant,  $r$  the bond length, and  $\gamma$  the bond-scaling parameter of order unity which is presumed to apply to *both* intramolecular and intermolecular forces. By superimposing such a microscopic  $k(r)$  scaling law on a very simple model for a molecular crystal, the overall aspects of the observed behavior under pressure are well reproduced. This elementary analysis reveals, in broad agreement with experiment, that the gross behavior of  $\gamma_i$  with  $\bar{\nu}_i$  is roughly  $\gamma_i \sim \bar{\nu}_i^{-2}$  and that the range of magnitudes spanned by the observed mode-Grüneisen parameters reflects the range of force constants characterizing the solid.

### I. INTRODUCTION

In comparison with the high level of detailed insight which has now been achieved for the forces which bind atoms together in covalent-network, ionic, and metallic crystals, the current understanding of the forces which hold together molecular crystals is relatively meager. Experimental probes of such forces are provided by spectroscopic techniques (Raman scattering, neutron scattering, far-infrared absorption) applied to lattice-dynamical studies of molecular solids, the low-frequency rigid-molecule (external) vibrations being of special interest here since their frequencies furnish a direct measure of the intermolecular forces.

During the past few years, the technique of pressure-Raman experimentation has been developed at several laboratories for investigating the effect on lattice frequencies of hydrostatic compression<sup>1-4</sup> and uniaxial stress.<sup>5</sup> While optical-pressure effects have long been used in studies of the electronic structure of solids,<sup>6</sup> their applications to lattice vibrations are very recent and have thus far been largely confined to the tetrahedrally coordinated, covalently bonded, network semiconductors of groups IV, III-V, and II-VI. Uniaxial stress experiments are impractical for molecular crystals, which are weak and easily crushed. Hydrostatic pressure, on the other hand, is an ideally suited external field to apply to such soft, highly compressible, solids. At 10 kbar, a typical

upper pressure attainable with fluid-medium hydraulic systems having optical access to the sample, molecular crystals experience a volume compression of 10% or more, compared to 1% for network crystals like Ge. Thus hydrostatic pressure provides a real opportunity to influence, and thereby investigate, the intermolecular "bonding" in molecular crystals.

This paper presents results of experiments on the effect of hydrostatic pressure on the first-order Raman-scattering spectra of two chalcogenide molecular crystals: orthorhombic sulfur ( $S_8$ ), a ring-molecule crystal; and orpiment ( $As_2S_3$ ), a layer crystal. Both crystals possess a large number of Raman-active zone-center optical phonons, so that a large number of mode-frequency pressure coefficients have been determined in this study. The results allow a detailed test of the Grüneisen scaling approximation

$$\Delta\bar{\nu}/\bar{\nu} = \gamma(-\Delta V/V), \quad (1)$$

where  $\Delta\bar{\nu}/\bar{\nu}$  is the fractional increase in the vibrational frequency of a crystal mode caused by a pressure-induced fractional volume decrease of  $-\Delta V/V$ . The experiments reported here reveal that, for molecular crystals, this frequency-volume scaling relation breaks down and *fails completely to describe the observed behavior*. Far from being constant, the mode-Grüneisen parameter is *strongly and systematically frequency dependent*;  $\gamma(\nu)$  varies by two orders of magnitude

as  $\bar{\nu}$  is varied over the phonon spectrum. This behavior is a consequence of the coexistence of strong intramolecular and weak intermolecular forces, and should prove characteristic of molecular crystals in general.

The structures of crystalline  $S_8$  and  $As_2S_3$  are discussed in Sec. II, experimental aspects are described in Sec. III, and the data are presented in Sec. IV. The observations are discussed in Sec. V in the context of some simple models and a bond-stiffness-bond-length scaling law consistent with the overall features of the experimental results. Principal findings of this work are summarized in Sec. VI.

## II. STRUCTURE AND BONDING OF $S_8$ AND $As_2S_3$

Molecular crystals are characterized by the coexistence of strong and weak interatomic forces; the strong forces bind together groups of atoms into well-defined molecular units, while the weak forces bind the molecules together to form the crystal. The degree to which this rough division into intramolecular and intermolecular "bonds" is valid depends on the disparity between their strengths (i. e., on the molecularity of the crystal); we shall accept its validity as a working assumption, providing support for it later in our discussion and analysis of the experimental results.

In both crystals which engage our attention here, the strong intramolecular bonding is covalent. The molecular unit in rhombic sulfur, a classic elemental molecular crystal, is an eight-membered square-antiprism puckered ring in which each atom is two fold coordinated. Two of the six  $3s^2 3p^4$  valence electrons of each sulfur atom enter into the covalent bonds with the two nearest neighbors, while the other four form two lone-pair orbitals which protrude into the intermolecular regions. The sulfur atoms in orpiment,  $As_2S_3$ , are similarly twofold coordinated, in this case to a pair of nearest-neighbor arsenics. The arsenic atoms are threefold coordinated, with the two leftover valence electrons (As is  $4s^2 3p^3$ ) forming a single lone-pair orbital. This threefold As coordination leads to the buildup of a two-dimensionally-extended, covalently connected network, producing a layer crystal in which the molecular unit is macroscopic in two dimensions. Noncoplanar and complex in structure, the layer may be approximately regarded as a pseudosandwich with the sulfur atoms forming the outside "surfaces." Thus the layer-layer intermolecular coordination in orpiment is primarily composed of sulfur-sulfur contacts, a key point of similarity to crystalline sulfur.

The crystal structures of rhombic sulfur<sup>7</sup> and of orpiment<sup>8,9</sup> are shown in Fig. 1. Both crystals are complex and of low symmetry. In sulfur there are

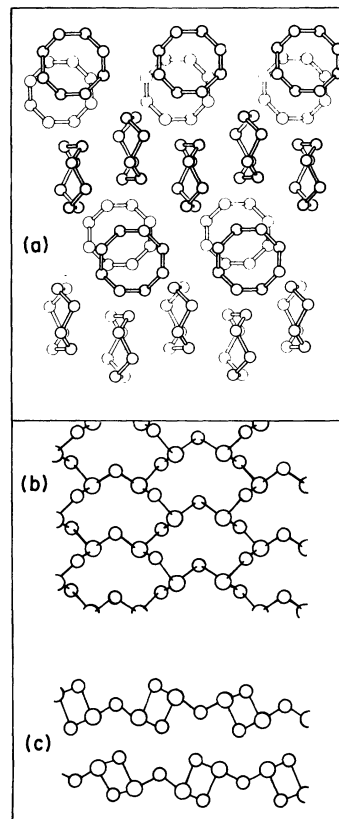


FIG. 1. Crystal structure of orthorhombic sulfur (a) and of orpiment (b) and (c). In (a) the sulfur structure is shown in a view perpendicular to the mean plane of half of the  $S_8$  rings. In (c) the  $As_2S_3$  structure is shown in a view looking at the layers edge on, while (b) shows a broadside view of a single layer.

four  $S_8$  molecules per unit cell, and the crystal symmetry is  $D_{2h}^{24}(Fddd)$ . Although, as an elemental crystal, rhombic sulfur is among the *chemically* simplest of molecular crystals, the *packing pattern* of the molecules in this condensed phase is quite intricate. The rings pack in staggered array to form two sets of nearly perpendicular columns, and these columns interweave each other log-cabin style as indicated in the figure.

In a layer crystal such as orpiment, the molecular packing axis is of course the normal to the layer mid-plane. With respect to translational invariance, the layer packing in  $As_2S_3$  is ... *ababab...*; i. e., two extended-layer molecules intersect the crystal unit cell. (We will abbreviate this statement by the phrase "two layers per unit cell.") The crystal unit cell contains 20 atoms (10 atoms per layer unit cell), and the crystal symmetry is  $C_{2h}^5(P2_1/n)$ . With two layers per unit cell,  $As_2S_3$  is of the *simplest type of layer crystal to exhibit optically-active rigid-layer phonons*.<sup>10</sup> This is relevant because such rigid-molecule modes directly mirror the intermolecular forces, so that

their behavior under pressure is of special interest.

### III. EXPERIMENTAL

Hydrostatic pressure was applied by means of a liquid hydraulic system using a 10-kbar one-stage hand pump of compact design due to Daniels.<sup>11</sup> The sample was contained in a three-window optical pressure cell which has been described by Brafman *et al.*<sup>1</sup> The pressure pump and optical bomb were connected by a now-standard method using flexible stainless-steel tubing.<sup>12</sup> The pressure-transmitting fluid was Octoil-S,<sup>13</sup> and the pressure was monitored with a manganin gauge<sup>14</sup> located in the pump. All of the high-pressure runs reported here were taken at room temperature.

Raman-scattering radiation was excited by a 30-mW He-Ne laser and spectrally analyzed by means of a Spex 1400 grating double monochromator and FW130 photomultiplier using dc detection. Both  $S_8$  (optical bandgap  $E_G = 3.1$  eV) and  $As_2S_3$  ( $E_G = 2.7$  eV) are transparent to He-Ne radiation ( $h\nu_L = 1.96$  eV) so that Raman emission could be observed in a right-angle configuration with the incident beam propagating through the bulk of the crystal. The laser beam entered the optical bomb along the vertical and the scattered radiation was collected along a horizontal axis.

The sulfur sample was a  $3 \times 3 \times 8$ -mm bar which was cut and polished from a large crystal grown (in the laboratory of W. Spear at Dundee)<sup>15</sup> by slow evaporation of a saturated solution in  $CS_2$ . Natural orpiment samples,<sup>9</sup> about 1 mm thick with  $5 \times 5$ -mm cleaved faces parallel to the layer planes, were employed with the laser beam impinging, at normal incidence, upon a cleaved face, and with the collected scattered radiation emerging from a narrow natural face oriented approximately  $70^\circ$  to the layer plane.

All of the many (over a dozen for each crystal) Raman lines investigated here were found to vary smoothly and reversibly, in frequency, as a function of pressure. No hysteresis effects were encountered in these hydrostatic experiments.

### IV. RESULTS

The low-frequency portion of the unpolarized Raman spectrum of sulfur is shown in Fig. 2 under normal conditions ( $T = 300^\circ\text{K}$  and  $P = 1$  atm  $\approx 0.00103$  kbar  $\approx 0.0$  kbar, henceforth referred to as zero-pressure conditions) and at 8.8 kbar. At zero pressure our results agree well with those of earlier studies.<sup>16,17</sup> The lines displayed in Fig. 2 nearly all correspond to external modes (rigid-molecule translations and rotations), and it is these frequencies which are most sensitive to pressure. All of the Raman lines of sulfur shift to higher frequency with increasing pressure. For

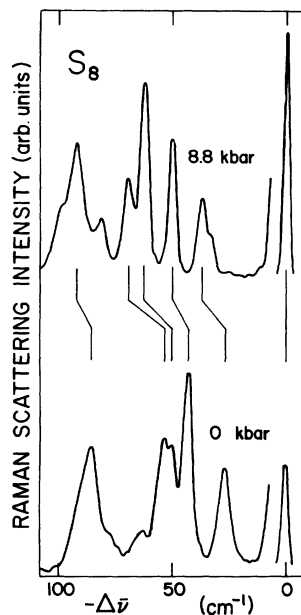


FIG. 2. Low-frequency portion of the sulfur Raman spectrum at low and high pressures.  $\Delta\bar{\nu}$  is the scattered photon's frequency shift from the He-Ne laser line at  $\bar{\nu}_L = 1.58 \times 10^4$   $\text{cm}^{-1}$ ; the phonon-emission ( $\Delta\bar{\nu} < 0$ ) Stokes spectrum is shown. Pressure-induced shifts to higher phonon frequency are indicated for several of the lines.

the low-frequency lines the relative shift is very large; for the lowest-lying line  $\Delta\bar{\nu}/\bar{\nu}$  amounts to some 40% in 9 kbar (which means that the effective force constant for this mode has *doubled* at this pressure).

Pressure-induced changes are most easily seen in the group of three lines located in the central part of Fig. 2. At zero pressure this trio consists of an intense singlet at  $43$   $\text{cm}^{-1}$  and a just-resolved doublet at  $51$ ,  $54.5$   $\text{cm}^{-1}$ . (Throughout this paper, phonon frequency  $\nu$  will be expressed in units of the wave-number equivalent  $\bar{\nu} = \nu/c$ .) The application of pressure causes these lines to spread quickly apart, with the doublet upshifting more rapidly than the singlet and also splitting so as to become very well resolved by 9 kbar. (This phenomenon of pressure-induced separation of closely spaced lines adds, in effect, a dimension of enhanced-resolution spectroscopy to optical-pressure experiments.) The attenuated laser line shown on the right-hand side of Fig. 2 indicates the spectral slit width of about  $2$ – $3$   $\text{cm}^{-1}$  full width at half-maximum. At  $P = 0$  the lowest-frequency line at  $26.5$   $\text{cm}^{-1}$  and the line at  $83.5$   $\text{cm}^{-1}$  appear appreciably broader than the instrument-limited laser line and the lines near  $50$   $\text{cm}^{-1}$ . At high pressure these lines reveal fine structure in the form of definite shoulders. While the  $83$ - $\text{cm}^{-1}$  band is known to be a multiplet from earlier high-resolution and low-temperature work,<sup>17</sup> these high-pressure data provide the first observation of any structure associated with the important  $26$ - $\text{cm}^{-1}$  line.

The observed pressure variation  $\bar{\nu}(P)$  of the Raman-active eigenfrequencies of sulfur is shown in Fig. 3. As seen in the right half of the figure,

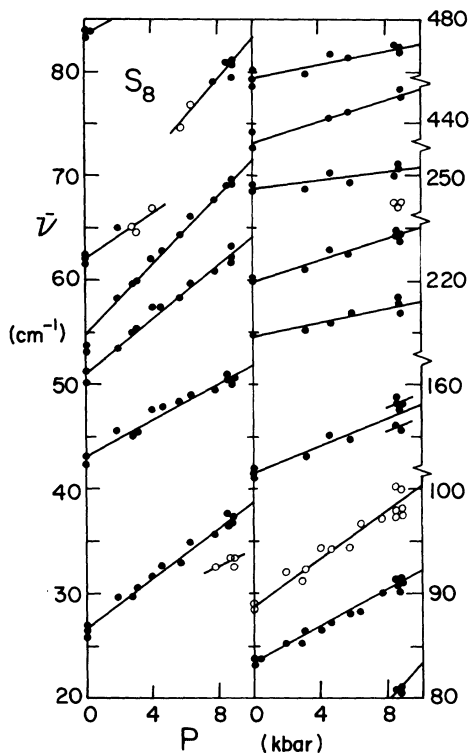


FIG. 3. Pressure dependence of Raman-active phonon frequencies in rhombic sulfur. Solid circles correspond to peak positions of strong or well-resolved Raman lines; open circles correspond to weak lines or shoulders.

the high-frequency modes upshift less rapidly with pressure than the low-frequency modes. As mentioned above, new lines are seen at high pressure. Besides the two cases near 26 and 83  $\text{cm}^{-1}$  (zero-pressure  $\bar{\nu}$ 's are given, unless stated otherwise), the lines at 152 and 249  $\text{cm}^{-1}$  reveal themselves as doublets at high pressure. A weak line at 62  $\text{cm}^{-1}$  disappears with pressure as it is overtaken by the strong 54- $\text{cm}^{-1}$  line, while the new line which appears in the vicinity of 80  $\text{cm}^{-1}$  ( $\bar{\nu}$  at  $P \approx 8$  kbar, the extrapolated zero-pressure  $\bar{\nu}$  is 65  $\text{cm}^{-1}$ ) is one whose intensity increases with pressure. All of the other lines observed appear at all pressures.

Perhaps the most interesting new feature in the high-pressure Raman spectrum of rhombic sulfur is the shoulder appearing a few  $\text{cm}^{-1}$  on the low-frequency side of the (initially) lowest line at 26  $\text{cm}^{-1}$ . We will immediately and briefly dispose of the discussion of this pressure-induced fine structure, since this aspect lies outside the main thrust of the discussion to follow. The low-frequency satellite of the 26- $\text{cm}^{-1}$  line is only tracked over a narrow range at the highest pressures shown in Fig. 3, so that no extrapolation to zero pressure is possible. It seems likely that the second mode is virtually degenerate with the 26- $\text{cm}^{-1}$  mode at

$P=0$ , since reported high-resolution low-temperature spectra show no structure in the lowest Raman line.<sup>17</sup> These very-low-frequency vibrations are rigid-molecule modes and most probably correspond to shear or rotational relative motions of adjacent  $S_8$  rings. There is no question here of a symmetry-induced degeneracy, since external modes belong to the crystal symmetry and  $D_{2h}$  symmetry is too low to call for such degeneracy. Besides, hydrostatic pressure leaves symmetry unaltered and so cannot lift a symmetry-induced degeneracy. A plausible possibility for a nearly-degenerate low-frequency doublet which splits under pressure would be a pair of vibrations composed of combinations of similar rigid-molecule motions on the two translationally inequivalent sets of columns (the stacks of  $S_8$  rings which comprise the "logs" of the log-cabin analog for the sulfur structure), if the coupling between these columns is weak and easily enhanced by pressure.

For orpiment, as for sulfur, our room-temperature zero-pressure spectra agree with earlier data.<sup>9</sup> Our results for the pressure dependence of the first-order Raman frequencies of crystalline  $As_2S_3$  are presented in Fig. 4. Again it is the low-frequency lines which are influenced most by crystal compression, while the highest-frequency in-

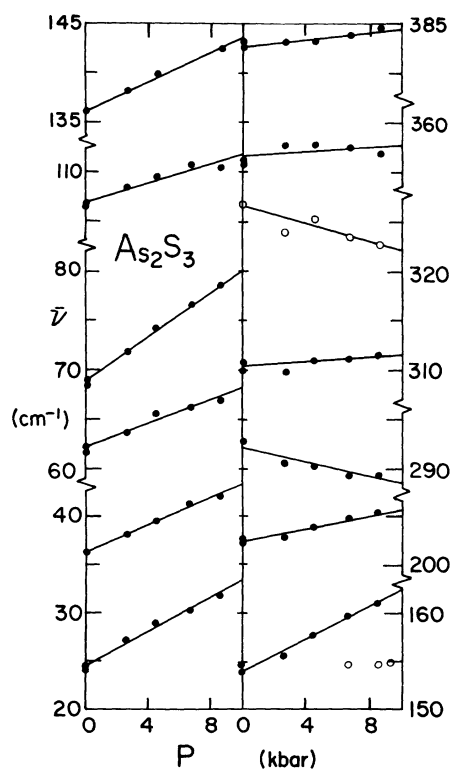


FIG. 4. Pressure dependence of Raman-active phonon frequencies in orpiment.

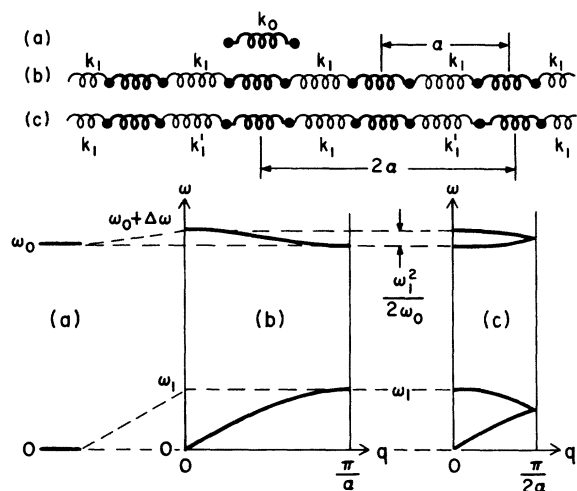


FIG. 5. Elementary vibrational models for molecular crystals: (a) free molecule, (b) linear lattice with one molecule per unit cell, (c) dimerized lattice with doubled unit cell. Corresponding phonon dispersion curves are displayed in the lower part of the figure.

ternal-mode (intralayer) lines are influenced least. For  $\text{As}_2\text{S}_3$  two of the Raman-active intralayer frequencies (293 and  $326\text{ cm}^{-1}$ ) actually go down as the pressure goes up.<sup>18</sup> At high pressure the  $154\text{-cm}^{-1}$  line reveals itself as a doublet. However the splitting of the  $356\text{-cm}^{-1}$  line (known to be a triplet from recent low-temperature work<sup>10,19</sup>) did not increase enough with pressure to be exposed in our medium-resolution experiments. In contrast to sulfur, the lowest-frequency Raman line in orpiment ( $25\text{ cm}^{-1}$ ) develops no subsidiary structure as it moves (rapidly) under pressure. This line, as will be discussed later, is produced by a nondegenerate shear-type rigid-layer vibration.

The pressure coefficients garnered from the slopes of the  $\bar{v}(P)$  lines of Figs. 3 and 4 are listed in Table I, along with the frequencies at  $P=0$ . In order to facilitate the discussion to come, the quantity tabulated is the logarithmic derivative  $d\ln\bar{v}/dP = (1/\bar{v})(d\bar{v}/dP)$ , expressed in units of  $10^{-2}\text{ kbar}^{-1}$  (i. e., in percent per kbar).

## V. DISCUSSION

### A. Molecular crystals: External and internal modes

In order to have in mind a basic framework in which to discuss our experimental results, we will consider the simplest conceivable vibrational model of a molecular crystal as illustrated in Fig. 5. This figure displays three one-dimensional spring models and their corresponding vibrational spectra (phonon dispersion curves). Figure 5(a) represents an isolated diatomic molecule (in a one-dimensional space) with atoms of mass  $m$  held to

their equilibrium separation by a spring of force constant  $k_0$ . The corresponding vibrational spectrum contains just two frequencies since there are but two degrees of freedom:  $\omega = \omega_0$ , where  $\omega_0 = (2k_0/m)^{1/2}$  is the frequency of the stretching mode; and  $\omega = 0$ , the vanishing frequency of the rigid-molecule free translation. In the model of Fig. 5(b) many such molecules are loosely bound together in a simple linear lattice (one molecule per unit cell) of periodicity  $a$ , weakly coupled by a set of soft intermolecular springs of force constant  $k_1$  ( $k_1 \ll k_0$ ). The frequency spectrum now spreads out into two bands  $\omega(q)$ ; the branches contained in the right half of the Brillouin zone ( $0 < q < \pi/a$ ) are shown in the central part of the lower half of Fig. 5. The  $\omega_0$  stretch vibration of the free molecule gives rise to a flat optical-phonon branch spanning the narrow frequency range from  $\omega_0$  (at the zone boundary) to  $\omega_0 + \Delta\omega$  (at the zone center). The  $\omega = 0$  free translation of the isolated molecule gives birth to the acoustic branch of the crystal, embracing low frequencies from 0 (at  $q=0$ ) to  $\omega_1$  (at  $q=\pi/a$ ). With  $k_1 \ll k_0$  the ratios of the characteristic frequencies of this elementary molecular lattice are given by

$$\omega_1/\omega_0 = (k_1/k_0)^{1/2}, \quad (2)$$

$$\Delta\omega/\omega_0 = \frac{1}{2}(k_1/k_0). \quad (3)$$

These relations illustrate the way in which both the flatness of the intramolecular-mode optical-phonon branch ( $\Delta\omega \ll \omega_0$ ) and the lowliness of the rigid-molecule-mode acoustic-phonon branch ( $\omega_1 \ll \omega_0$ ) depend upon the weakness of the intermolecular bonding ( $k_1 \ll k_0$ ). Considering  $\epsilon = (k_1/k_0)^{1/2}$  as a parameter of smallness in the weak-coupling limit, (2) and (3) show that  $\omega_1$  is of first order in  $\epsilon$  while  $\Delta\omega$  is of second order.

As a slight concession in the direction of the complexity of real crystals, the next stage of complication is introduced in Fig. 5(c) by doubling the unit-cell size to include two molecules. This minimal complexity is useful for making contact with spectroscopy since the unit-cell doubling places the coupling effects ( $\omega_1, \Delta\omega$ ) at the zone center (where they must be in order to be accessible to first-order Raman-scattering or far-infrared experiments). In the model of Fig. 5(c) the pairing-off (dimerization) is effected by letting alternate intermolecular force constants adopt a value  $k'_1$  slightly different from  $k_1$ . The phonon spectrum is essentially similar to that of Fig. 5(b) but with the original Brillouin zone folded back upon itself, since a doubling in real space corresponds to a halving in reciprocal space.

The main qualitative spectral features which appear when the intermolecular interaction is turned

on can be seen by comparing the  $q=0$  phonon spectrum of Fig. 5(c) with the noninteracting-molecule spectrum of Fig. 5(a). In the crystal there appear very-low-frequency rigid-molecule modes ( $\omega_1$ ), and Davydov-splitting fine structure ( $\Delta\omega$ ) is imposed on the intramolecular modes ( $\omega_0$ ). Both types of spectral features can be used, via relations corresponding to (2) and (3), to estimate the strength of the intermolecular forces. This has been done in our earlier studies<sup>9,10</sup> of  $\text{As}_2\text{S}_3$ , as will be discussed in Sec. V.

The distinction between intramolecular and rigid-molecule (i. e., between internal and external) vibrational modes is a useful concept and an excellent approximation<sup>20</sup> for most of the modes, but it becomes a bit blurred for very complex molecular crystals in which the profusity of frequencies tends to fill in the gap between the lowest of the  $\omega_0$ 's and the highest of the  $\omega_1$ 's. The  $D_{4d}$ -symmetry  $S_8$  molecule possesses 11 intramolecular eigenfrequencies (7 of them Raman-active) spanning the range from 475 down to 85  $\text{cm}^{-1}$ . With four molecules per unit cell there are 21 ( $4 \times 6 - 3$ ) translational-librational rigid-molecule  $q=0$  optical modes (12 of them Raman-active) crowded into the frequency regime below about 65  $\text{cm}^{-1}$ . Thus the internal/external demarcation boundary in sulfur is at about 75  $\text{cm}^{-1}$ .

In orpiment there are more intramolecular and fewer intermolecular eigenfrequencies than in sulfur. In a layer crystal the external modes are rigid-layer translations,<sup>10</sup> and with two layers per crystal unit cell there are three rigid-layer zone-center optical phonons. ( $\text{As}_2\text{S}_3$  thus corresponds to the layer-crystal analog of Fig. 5(c), the *minimum-complexity* situation for occurrence of  $q=0$  rigid-molecule optical phonons.) Because of the low ( $C_{2h}^5$ ) crystal symmetry, the three rigid-layer eigenfrequencies are all nondegenerate and Raman-active. Internal (intralayer) modes in a layer crystal are determined by the layer unit cell and the diperiodic space-group symmetry of the individual extended layer<sup>9,21,22</sup>; in  $\text{As}_2\text{S}_3$  the layer unit cell contains ten atoms and the layer (diperiodic) symmetry is  $C_{2v}^7$ . All 27 intralayer vibrations are nondegenerate and Raman active. There are therefore 27 possible internal-mode Raman in addition to the three external-mode Raman lines. The intralayer eigenfrequencies extend from nearly 400  $\text{cm}^{-1}$  down to about 60–70  $\text{cm}^{-1}$ . A recent analysis<sup>10</sup> indicates that two of the rigid-layer modes correspond to the 25- and 36- $\text{cm}^{-1}$  Raman lines, but that the third is appreciably admixed with an intralayer mode near 60  $\text{cm}^{-1}$ . Thus in orpiment the internal/external demarcation frontier occurs in a frequency region similar to that obtained in sulfur, but in  $\text{As}_2\text{S}_3$  it appears that this no-mans-land in frequency space is populated by a few vibrations quite mixed in character.

#### B. Effect of pressure: Phenomenological scaling and the Grüneisen approximation

Application of external pressure to a lattice held together by perfect springs would compress the crystal volume but leave all phonon frequencies unaltered, since the force constants holding the atoms to their new (more closely spaced) equilibrium positions would be the same as before. In actual crystals, of course, vibrational eigenfrequencies *do* change under pressure (e. g., Figs. 2–4), almost always increasing with compression because interatomic and intermolecular bonds stiffen as they shorten. A convenient way of expressing this anharmonicity effect on a given mode frequency is in terms of a dimensionless quantity directly related to the observed pressure coefficient:

$$\gamma_i = -\frac{V}{\bar{\nu}_i} \frac{d\bar{\nu}_i}{dV} = -\frac{d \ln \bar{\nu}_i}{d \ln V} = \frac{1}{\kappa} \frac{d \ln \bar{\nu}_i}{dP}. \quad (4)$$

$\gamma_i$  is the mode-Grüneisen parameter for phonon  $i$ ,  $V$  the crystal volume,  $P$  the pressure, and  $\kappa$  the compressibility. Weighted averages (over  $i$ ) of  $\gamma_i$  enter into theories of the thermal expansion and the equation of state of solids.<sup>23</sup> For example, in order to construct a simple theory of thermal expansion, Grüneisen assumed all of the  $\gamma_i$  to be equal.<sup>24</sup> In this approximation the coefficient of thermal expansion  $\alpha$  is given by  $\gamma \kappa c_v$ , directly proportional to the Grüneisen constant (as well as to the compressibility and the specific heat at constant volume).

For three-dimensional-network crystals such as Ge and NaCl (each atom connected to every other by paths of strong interatomic interactions) the Grüneisen approximation is a useful idea of reasonable validity. Optical phonons in the germanium-family covalently bonded group-IV and group-III-V semiconductors exhibit Grüneisen  $\gamma$ 's close to unity.<sup>2-5,25</sup> In the II-VI semiconductors the pressure dependence of optical-phonon frequencies typically correspond to a  $\gamma_i$  of about 2,<sup>2-5</sup> while in the alkali halides  $\gamma_i$  is about 3.<sup>26</sup> (Correlation between  $\gamma_i$  and ionicity has been pointed out by Mitra and Brafman.<sup>2,3</sup>) In most of these simple non-molecular crystals the unit cell is small and symmetric so that only a single  $q=0$  optical phonon can be followed in a pressure-Raman or pressure-infrared experiment. An interesting exception is TlI, an ionic crystal with a somewhat more complex structure for which five Raman-active phonons have been tracked with pressure.<sup>1</sup>  $\gamma_i$  is approximately the same for all five modes ( $\gamma_i \approx 3$ , which is also the value of  $\alpha/\kappa c_v$  for this crystal).

From prior experience then (largely confined, as briefly synopsized above, to network crystals), it might have been supposed that the numerous

optically accessible phonon frequencies of  $S_8$  and  $As_2S_3$  would exhibit stress-induced shifts corresponding to  $\gamma$ 's of order unity. Thus  $d\bar{\nu}/dP$  would be expected to be proportional to  $\bar{\nu}$ . That this is *not* the case, and by a wide margin, is evident in a glance at Figs. 3 and 4. Not only is the pressure coefficient  $d\bar{\nu}/dP$  not proportional to  $\bar{\nu}$ , but it actually *decreases* with increasing frequency!

The experimental results for the rates of change of frequency with pressure have been given in Table I in the form of the fractional change per increment of pressure,  $d \ln \bar{\nu}_i / dP$ , in units of percent per kbar or  $10^{-2} \text{ kbar}^{-1} = 10^{-5} \text{ bar}^{-1}$ . To convert, via (4), this logarithmic pressure coefficient (of frequency) to  $\gamma$ , a volume coefficient, requires the compressibility  $\kappa$ . For both  $S_8$ <sup>27</sup> and  $As_2S_3$ <sup>28</sup> it happens that  $\kappa$  is close to  $1.0 \times 10^{-5} \text{ bar}^{-1}$ , so that the corresponding  $\gamma_i$ 's are approximated by the numerical values listed in the table.

While the pronounced inconstancy of  $\gamma_i$  is obvious from Table I, the clearest demonstration of this is in a plot of  $\gamma_i$  vs  $\bar{\nu}_i$ , a representation of the data which should yield a horizontal line in the Grüneisen approximation. Such a plot (in log-log form) has been constructed in Fig. 6. Each point in this figure corresponds to a Raman-active zone-center phonon in sulfur or in arsenic sulfide,

TABLE I. Logarithmic pressure coefficients<sup>a</sup> of Raman-active phonons<sup>b</sup> in  $S_8$  and  $As_2S_3$ .

Sulfur		Orpiment	
$\bar{\nu}_i$ ( $\text{cm}^{-1}$ )	$(1/\bar{\nu}_i)(d\bar{\nu}_i/dP)$ ( $10^{-2} \text{ kbar}^{-1}$ )	$\bar{\nu}_i$ ( $\text{cm}^{-1}$ )	$(1/\bar{\nu}_i)(d\bar{\nu}_i/dP)$ ( $10^{-2} \text{ kbar}^{-1}$ )
26.5	4.5	25	3.6
43	2.0	36	2.0
51	2.5	62	0.80
54.5	3.1	69	1.6
62	1.7	107	0.46
65 <sup>c</sup>	2.8	136	0.54
83.5	1.05	154	0.55
89	1.26	202	0.16
152	0.43	292	-0.13
215	0.15	310	0.034
220	0.23	326	-0.14
249	0.08	357	0.027
438	0.10	383	0.044
474	0.067		

<sup>a</sup>Estimated experimental errors for the observed values of  $d \ln \bar{\nu}_i / dP$  are about 5% for the pressure coefficients of the Raman frequencies below 60 (70)  $\text{cm}^{-1}$  for  $S_8$  ( $As_2S_3$ ), about 15% for the coefficients of the frequencies above 150 (300)  $\text{cm}^{-1}$  for  $S_8$  ( $As_2S_3$ ), and about 10% for the rest of the lines listed.

<sup>b</sup>The zero-pressure Raman frequencies listed are accurate to  $\pm 1 \text{ cm}^{-1}$ .

<sup>c</sup>This is the extrapolated  $P=0$  frequency for a line seen only at high pressure.

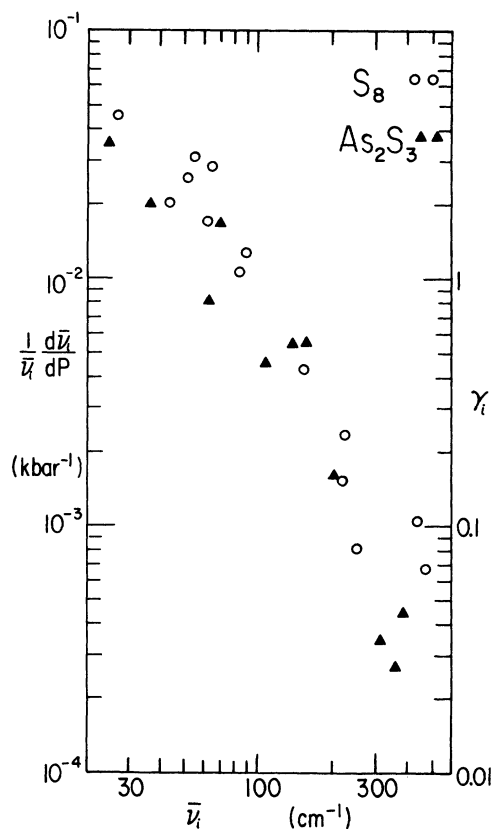


FIG. 6. Correlation between mode-Grüneisen parameter and phonon frequency for the molecular crystals sulfur and orpiment.

with the horizontal coordinate fixed by the zero-pressure value of frequency and the vertical coordinate fixed by the logarithmic pressure coefficient of the frequency as observed in our pressure experiments. (The two negative coefficients seen in  $As_2S_3$  are omitted from the figure.)  $\gamma$ , as well as  $(1/\bar{\nu})(d\bar{\nu}/dP)$ , labels the vertical scale in Fig. 6.

Far from being frequency independent,  $\gamma(\bar{\nu})$  varies sharply—by two orders of magnitude—over the frequency spectrum. Moreover this variation is very systematic, with  $\gamma$  decreasing with increasing  $\bar{\nu}$ . Only at the smallest  $\bar{\nu}$ 's is  $\gamma$  of order 1;  $\gamma$  is much less than unity at large  $\bar{\nu}$ . We believe that such a strongly-frequency-dependent mode-Grüneisen parameter, with  $\gamma$  plummeting as a function of  $\bar{\nu}$ , will prove to be a general property of molecular crystals. A simple argument for this will now be discussed, in the context of the rudimentary molecular-crystal model of Fig. 5.

The Grüneisen approximation, in which Eq. (1) is taken to apply to all of the vibrational frequencies ( $\gamma_i = \gamma$ , independent of  $i$ ), amounts to a phenomenological scaling law connecting phonon frequency

with crystal volume:

$$\bar{v} \approx (\text{const.}) \times V^{-\gamma}. \quad (5)$$

This in turn implies that the force constants scale with volume as

$$k \approx (\text{const.}) \times V^{-2\gamma}. \quad (6)$$

While approximation (5) attains some success for three-dimensional-network crystals held together by a single type of bond, we have seen that it fails dramatically for crystals in which there coexist several types of bonds of widely disparate strengths.

Although the uniform spectral expansion of (5) does *not* accompany the spatial compression of a molecular crystal, we may adapt the more general force-constant scaling of (6) to address a situation characterized by both strong and weak bonds. Underlying the latter scaling law is the dependence of force constant  $k$  upon bond length  $r$ . The bond-stiffness-bond-strain relation corresponding to (6) is

$$k \approx (\text{const.}) \times r^{-6\gamma}. \quad (7)$$

The empirical power-law form of (7) for  $k(r)$  has been induced, via (5), from situations dominated by a single bond type.<sup>29</sup> In such solids the bonds opposing pressure-induced volume compression are necessarily the same as those providing the restoring forces for the crystal eigenvibrations. This is not so when bonds of disparate strengths are present, and we have seen that (5) doesn't work (i. e., no single value of  $\gamma$  even approximately fits  $\bar{v}_i$  vs  $V$ ) in molecular solids. Let us suppose, however, that each bond type  $j$  *individually* obeys a scaling law  $k_j(r_j)$  of the form of (7), and that each such bond-strength-bond-length relation *has the same*  $\gamma$  of order unity. We then find that this assumption leads to  $\bar{v}_i(V)$  scaling consistent with the observations of Fig. 6.

To see this we consider the basic model of Fig. 5(o). The differential statements of (7) for the intramolecular ( $k_0$ ) and intermolecular ( $k_1$ ) force constants are given by

$$\Delta k_0/k_0 = -6\gamma \Delta r_0/r_0 = -6\gamma_0 \Delta a/a, \quad (8a)$$

$$\Delta k_1/k_1 = -6\gamma \Delta r_1/r_1 = -6\gamma_1 \Delta a/a. \quad (8b)$$

The quantities  $\gamma_0$  and  $\gamma_1$  defined by (8) specify the connections between the bond stiffnesses and the overall *macroscopic* strain  $\Delta a/a$  ( $a = r_0 + r_1$ ), so that it is these  $\gamma$ 's (and not the microscopic scaling parameter  $\gamma$ ) which correspond to the observed mode-Grüneisen parameters of Eq. (4). Thus although it has been taken that the same scaling exponent ( $-6\gamma$ ) appears in both  $k_0(r_0)$  and  $k_1(r_1)$ , the upshot will be very different exponents for the experimentally accessible functions  $k_0(a)$  and  $k_1(a)$ . This difference follows directly from the disparity

of the bond stiffnesses: The intermolecular volume ( $\sim r_1$  in the one-dimensional model) is clearly much more compressible than the intramolecular volume ( $\sim r_0$ ).

We will refer to  $\gamma$ , the bond-stiffness-bond-length scaling parameter of (7) (which has been presumed to apply to both intramolecular and intermolecular bonds), as the bond-scaling parameter. This quantity, of more basic significance than the observed frequency-volume mode-Grüneisen parameters  $\gamma_i$ , will henceforth be distinguished from the latter by the absence of the optical-phonon subscript  $i$ . This distinction is unimportant for network crystals since  $\gamma_i \approx \gamma$ . But for molecular crystals the distinction is essential because for these solids  $\gamma_i$  is largely decoupled from  $\gamma$  and can take on values as much as two orders of magnitude different. The point is that even with the enormous variability of the measured values of mode-Grüneisen parameters, as seen in Fig. 6, the bond-scaling parameter allows us to preserve for molecular solids, *the notion of a vibrational scaling-law "constant" of order unity.*

Following (8), the mode-Grüneisen  $\gamma$ 's for modes  $\omega_0$  and  $\omega_1$  of the linear molecular lattice are simply evaluated in terms of the bond-scaling  $\gamma$ :

$$\gamma_0 = \gamma(1 + r_1/r_0)(1 + k_0/k_1)^{-1} \approx \gamma(1 + r_1/r_0)(k_1/k_0), \quad (9a)$$

$$\gamma_1 = \gamma(1 + r_0/r_1)(1 + k_1/k_0)^{-1} \approx \gamma(1 + r_0/r_1). \quad (9b)$$

The approximate expressions on the right-hand side of (9) invoke  $k_1 \ll k_0$ . The second term in each of these expressions depends on geometry; if we assume, for concreteness, comparable intramolecular and intermolecular volumes ( $r_0 \approx r_1$  in this one-dimensional case), we arrive at the following crude but instructive results:

$$\gamma_0 \approx (k_1/k_0) 2\gamma, \quad (10a)$$

$$\gamma_1 \approx 2\gamma. \quad (10b)$$

While the rigid-molecule mode  $\omega_1$  exhibits a mode-Grüneisen parameter  $\gamma_1$  which is of the same order as  $\gamma$  (somewhat larger, in fact, owing to the geometrical factor which is the ratio of the total volume to the intermolecular volume) and is thus of order 1 and of "normal" size, the internal mode  $\omega_0$  yields a value  $\gamma_0$  which is depressed by the intermolecular-intramolecular force-constant ratio and is therefore "anomalously" small. These qualitative conclusions are preserved in the analysis of analogous three-dimensional models in which the intramolecular and intermolecular volumes are comparable and their corresponding compressibilities are  $\kappa_0$  and  $\kappa_1 \approx (k_0/k_1)\kappa_0$ . With these approximations valid the three-dimensional results for  $\gamma_i$  are identical to (10).

A sketch of the implications of this discussion is



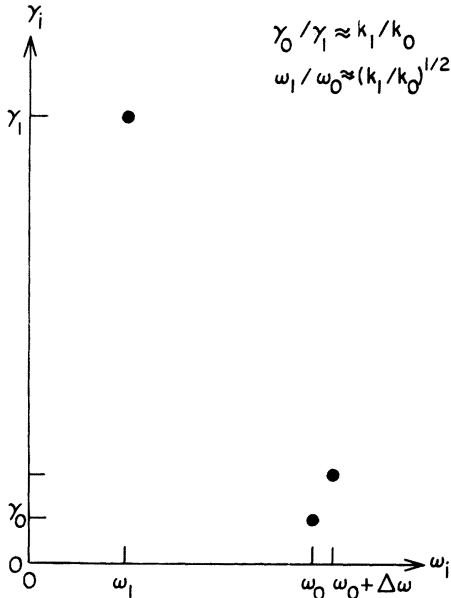


FIG. 7. Bond-scaling results for pressure effects on  $q=0$  optical phonons in the model of Fig. 5(c).

shown in Fig. 7, in which  $\gamma_i(\omega_i)$  is indicated for each of the three zone-center optical phonons of Fig. 5(c). The  $\gamma_i$ 's for  $\omega_0$  and  $\omega_1$  are based on (10) with  $\gamma$  set equal to 1, and  $\gamma_i$  for the upper optical phonon at  $\omega_0 + \Delta\omega$  is obtained by similar arguments.  $\gamma_i(\omega_0 + \Delta\omega)$  exceeds  $\gamma_i(\omega_0)$  because compression not only lifts the optical-phonon band but also spreads the band by increasing the intermolecular-interaction Davydov splitting  $\Delta\omega$ .

### C. Hierarchy of forces

The rudimentary treatment given above implies, via expressions (10) and Fig. 7, a wide range of frequency-volume mode-Grüneisen parameters extending from  $\gamma_i \sim 1$  for external modes down to  $\gamma_i \sim k_1/k_0$  for internal modes. The observed  $\gamma_i(\bar{\nu}_i)$ 's of Fig. 6 do indeed clearly exhibit a steep falloff between low and high frequencies, in broad agreement with the simple analysis. This decline is quite systematic and proceeds continuously without any clear discrete transition from an intermolecular to an intramolecular regime.

The absence of any definite marker in  $\gamma_i(\bar{\nu}_i)$  must originate from the same reasons as those underlying the absence of any appreciable frequency gap separating external and internal modes in the overall  $q=0$  vibrational spectrum of both sulfur and orpiment. Even if we were to cling to the oversimplified idea of just two characteristic force constants as in Fig. 5, the geometrical complexity and spectral richness of these crystals would allow intermediate frequencies between  $\bar{\nu}_1$  and  $\bar{\nu}_0$

and intermediate mode-Grüneisen  $\gamma_i$ 's between  $\gamma_1$  and  $\gamma_0$  to be fairly densely filled in by the many possible admixtures of  $k_0$  and  $k_1$ . Of course, even in a simple valence force picture of the solid there are force constants in addition to the two principal bond-stretching ones for strong and weak bonds. Thus the covalently bonded molecular units in  $S_8$  and  $As_2S_3$  feature bond-bending force constants  $k'_0$  which, in appropriate units, are intermediate between  $k_0$  and  $k_1$  (though closer to the former). Likewise there are intermolecular shear or bond-bending forces (such as, *inter alia*, those responsible for providing the very weak restoring forces for the shear-type rigid-layer vibrations in graphite) which can be parameterized by corresponding quantities  $k'_1$ . The hierarchy of forces can be expressed as  $k_0 > k'_0 > k_1 > k'_1$ .

In the spirit, adopted throughout this paper, of developing a simplified viewpoint to deal with the overall behavior, we shall attack the above complications by attaching, to each mode  $i$ , an effective force constant  $k_i$  produced by the interplay of the various forces. Over the vibrational spectrum we can expect  $k_i$  to run the gamut from  $k'_1$  to  $k_0$ . For  $As_2S_3$  the analysis<sup>10</sup> of rigid-layer and intralayer phonon frequencies yields  $k'_1/k_0 = 0.017$ , so that  $k_i$  possesses a scope of nearly two orders of magnitude. Since  $\bar{\nu}_i \sim k_i^{1/2}$  and since, from (10),  $\gamma_i \sim k_i^{-1}$ , the optical-phonon frequencies should span a factor of about 10 while the mode-Grüneisen constants span, with opposite sense, a factor of about 100. This is just the observed behavior of Fig. 6. Moreover, eliminating  $k_i$  from these relations yields a rough guide for the  $\gamma_i(\bar{\nu}_i)$  correlation between mode-Grüneisen parameter and mode frequency in a molecular crystal:

$$\gamma_i \sim \bar{\nu}_i^{-2}. \quad (11)$$

Though crude, (11) is quite consistent with the gross behavior exhibited in Fig. 6 and therefore appears to be a useful approximation for the connection between the vibrational frequency and its observed sensitivity to changes in volume.

### D. Scaling of bond stiffnesses

We have now seen, by means of the good correlation between (10) and (11) on the one hand with the pressure-Raman data of Fig. 6 on the other, that the bond-strength-bond-length power-law scaling of (7), with a bond-scaling  $\gamma$  close to unity, successfully describes the situation for the two molecular crystals investigated here. Thus although we are forced to abandon, for molecular solids, the usual frequency-volume form of the Grüneisen approximation as stated in (5), we can yet retain the deeper and more general expression of this idea which is embodied in the stiffness-strain relation  $k \sim r^{-6\gamma} \sim r^{-6}$ .

Although it fails badly overall, the  $\bar{\nu} \sim V^{-1}$  form does describe the behavior of a few intermolecular modes. Actually for the lowest-frequency modes observed in sulfur and arsenic trisulfide,  $\gamma_i$  is larger than 1 ( $\approx 4$ ). One reason for this, already discussed, is that the intermolecular volume experiences a relative compression somewhat exceeding that of the total volume; this geometrical consideration introduced the factor of 2 in expression (10b). There is an additional consideration for the very lowest in frequency of the optical modes. A  $\gamma_i$  of order 1 corresponds to a situation in which the bonds opposing the volume compression, i. e., which determine  $\kappa$ , are the same as those providing the vibrational restoring force (as is the case for optical modes in network crystals). Now while the volume contraction in a molecular crystal under hydrostatic pressure is soaked up mainly by compressed intermolecular bonds ( $k_1$ ), the smallest  $\bar{\nu}_i$ 's primarily reflect intermolecular shear forces ( $k_1'$ ). The corresponding  $\gamma_i$ 's should thus be enhanced by an additional factor  $k_1/k_1'$ .

Throughout this paper the length-strength relationship of (7) has been applied separately to each type of bond in order to describe the  $k_j(r_j)$  scaling for that bond type, and this has been sufficient for the discussion of our pressure experiments. At this point we shall not resist the temptation to point out the possibility of an analogous relationship cutting across the lines which separate intramolecular and intermolecular bonds. In Table II we have listed values of  $r_1/r_0$  (intermolecular-intramolecular closest separations) and  $k_1/k_0$  deduced for  $\text{As}_2\text{S}_3$  and several other layer crystals from a recent analysis of the rigid-layer optical phonons in these crystals.<sup>10</sup> If we suppose that  $k \sim r^{-n}$  can be naively applied to these data by adopting not only the same exponent  $n$  but also the same prefactor for both  $k_0(r_0)$  and  $k_1(r_1)$ , we obtain the values of  $n$  given in the last column of the table. It is provocative that these values (obtained by comparing different bond types) are not very different from  $n=6$ , varying between 5 and 8; this of course corresponds in (7) to a microscopic

bond-scaling parameter of  $\gamma \approx 1$ , as required (for each individual bond type) by the pressure results. It has previously been suggested<sup>9</sup> that the intermolecular interaction in  $\text{As}_2\text{S}_3$  contains an appreciable admixture of weak covalent bonding (rather than consisting predominantly of van der Waals forces, as is usually uncritically assumed for molecular crystals in the absence of better information), and the present results tend to support this view.

#### E. Anharmonicity

Grüneisen parameters are inextricably connected with anharmonicity effects, a point which has not been explicitly emphasized here but which calls for a brief comment. The degree to which interatomic force constants depend upon strain is precisely the degree to which the harmonic approximation for lattice dynamics fails to apply. The clearest illustration of  $\gamma$  as an anharmonicity-induced response function is via a simple example. Consider a simple-cubic network crystal with only nearest-neighbor interactions represented by atom-atom bonds of equilibrium length  $r_0$  and of potential energy  $\frac{1}{2}k_0r_0^2(\Delta r/r_0)^2 - k_0^{(3)}r_0^3(\Delta r/r_0)^3$ . Here  $\frac{1}{2}k_0$  and  $k_0^{(3)}$  are, respectively, the quadratic and cubic coefficients in the expansion of the potential in powers of the bond stretch  $\Delta r = r - r_0$ . For such a system it is easily shown that pressure causes each phonon frequency to shift with volume compression as  $\Delta\bar{\nu}/\bar{\nu} = -\gamma(3\Delta r/r_0)$ , with the Grüneisen constant (identical in this case to the bond-scaling parameter) given by  $\gamma = k_0^{(3)}r_0/k_0$ . This simple expression transparently exposes the proportionality of  $\gamma$  to higher-than-second derivatives of the potential; general expressions have been constructed by Ganesan *et al.*<sup>30</sup> for diamond-structure crystals.

Having pointed out the proportionality of  $\gamma$  to anharmonicity, a quick caveat is in order for the intramolecular modes. It would of course be a mistake to conclude from their miniscule  $\gamma_i$ 's that in molecular crystals the internal vibrations experience remarkably little anharmonicity. The relevant quantity here is not the observed  $\gamma_i$ , which is tiny because the molecular volume is so incompressible in comparison to the crystal volume, but the bond-scaling  $\gamma$  of (7), which is of normal size for the internal modes just as it is for the external modes. It is interesting to note that such "normal" anharmonicity, associated with the apparent universality of  $\gamma \approx 1$ , implies (from the identification of  $\gamma$  with  $k_0^{(3)}r_0/k_0$ ) that anharmonic coefficients in the expansion of the potential are typically of just the magnitude which would allow the anharmonic terms to overtake the harmonic terms in size at the (unreachable) strain of about 100% ( $|\Delta r/r_0| = 1$ ).

TABLE II. Interlayer-to-intralayer force-constant ratios in several layer crystals.<sup>a</sup>

Crystal	$r_1/r_0$	$k_1/k_0$	$n$ (if $k_j = cr_j^{-n}$ )
$\text{As}_2\text{S}_3$	1.55	0.06	6.4
$\text{As}_2\text{Se}_3$	1.51	0.07	6.5
GaSe	1.6	0.07	5.6
$\text{MoS}_2$	1.5	0.038	8.1
Graphite	2.36	0.010	5.4

<sup>a</sup>These data are taken from the systematic analysis of rigid-layer and intralayer vibrational frequencies carried out in Ref. 10.

## VI. SUMMARY

The effect of pressure on lattice vibrations in two molecular crystals, the ring-molecule elemental crystal orthorhombic sulfur and the layer-structure chalcogenide crystal  $\text{As}_2\text{S}_3$ , has been measured by observations of their first-order Raman-scattering spectra at pressures to 10 kbar. The experimental results on the many Raman-active modes in these crystals, as shown in Figs. 2-4 and, especially, Fig. 6, reveal that (in contrast to network crystals) the compression-induced shifts of the optical-phonon frequencies in molecular crystals are strikingly inconsistent with the usual frequency-volume Grüneisen scaling law. Far from being frequency independent, the mode-Grüneisen parameter  $\gamma_i = (\Delta\bar{\nu}_i/\bar{\nu}_i)(-\Delta V/V)^{-1}$  varies sharply and systematically with mode frequency  $\bar{\nu}_i$  over the optical-phonon spectrum, falling steeply from values of order 1 at low frequencies to values of order  $10^{-2}$  at high frequencies.  $\gamma_i$  is thus of "normal" size for external modes but is "anomalously" small for internal modes.

Although the approximate scaling relation  $\bar{\nu}_i \sim V^{-\gamma}$  (with  $\gamma \approx 1$  for all  $i$ ) must be abandoned for molecular crystals, the notion of a vibrational scaling law in the Grüneisen spirit can be preserved in the form of the more basic bond-stiffness-bond-length scaling relation  $k \sim r^{-6\gamma}$ . Here  $k$  is the force constant,  $r$  the bond length, and  $\gamma$

the bond-scaling parameter of order unity which is presumed to apply to *both* intramolecular and intermolecular forces. By superimposing such a microscopic  $k(r)$  relation on a simple model of a molecular crystal (Fig. 5), we have reproduced [Eqs. (8)-(11), Fig. 7] the overall aspects of the observed behavior under pressure. This elementary analysis reveals that the gross behavior of  $\gamma_i$  with  $\bar{\nu}_i$  is roughly  $\gamma_i \sim \bar{\nu}_i^{-2}$ , and that the range of magnitudes spanned by the observed mode-Grüneisen parameters reflects the range of force constants characterizing the solid. These broad features, observed here for sulfur and orpiment, should prove to be characteristic aspects of the influence of pressure on the vibrational spectra of all molecular crystals.

## ACKNOWLEDGMENTS

The experiments reported in this paper were performed while the author was a visitor on the faculty of the Solid State Institute, The Technion-Israel Institute of Technology, Haifa, Israel. It is a pleasure to express appreciation for the splendid hospitality of Oren Brafman and Elisha Cohen, in whose laboratory this work was performed, and for the expert help of Michael Hayek, Chanoch Katz, and Micki More in the performance of some of these experiments.

\*Permanent address.

<sup>1</sup>O. Brafman, S. S. Mitra, R. K. Crawford, W. B. Daniels, C. Postmus, and J. R. Ferraro, *Solid State Commun.* **7**, 449 (1969).

<sup>2</sup>S. S. Mitra, O. Brafman, W. B. Daniels, and R. K. Crawford, *Phys. Rev.* **186**, 942 (1969).

<sup>3</sup>O. Brafman and S. S. Mitra, in *Proceedings of the International Conference on Light Scattering in Solids, Paris, 1971*, edited by M. Balkanski (Flammarion, Paris, 1971), p. 284.

<sup>4</sup>C. J. Buchenauer, F. Cerdeira, and M. Cardona, in *Ref. 3*, p. 280.

<sup>5</sup>F. Cerdeira, C. J. Buchenauer, F. H. Pollak, and M. Cardona, *Phys. Rev. B* **5**, 580 (1972).

<sup>6</sup>W. Paul, in *Proceedings of the Enrico Fermi Summer School on Optical Properties of Solids, Varenna, 1965*, edited by J. Tauc (Academic, New York, 1966), p. 257.

<sup>7</sup>J. Donahue, in *Elemental Sulfur*, edited by B. Meyer (Interscience, New York, 1965), p. 13; R. W. G. Wyckoff, *Crystal Structures* (Interscience, New York, 1963), Vol. 1, p. 33.

<sup>8</sup>N. Morimoto, *Mineral. J. (Sapporo)* **1**, 160 (1954).

<sup>9</sup>R. Zallen, M. L. Slade, and A. T. Ward, *Phys. Rev. B* **3**, 4257 (1971).

<sup>10</sup>R. Zallen and M. L. Slade, *Phys. Rev. B* **9**, 1627 (1974).

<sup>11</sup>W. B. Daniels, *Rev. Sci. Instr.* **37**, 1502 (1966).

<sup>12</sup>W. Paul and D. M. Warschauer, *Rev. Sci. Instr.* **27**, 418 (1956).

<sup>13</sup>W. B. Daniels and A. A. Hruschka, *Rev. Sci. Instr.*

**28**, 1058 (1957).

<sup>14</sup>P. W. Bridgman, *The Physics of High Pressure* (Bell, London, 1958).

<sup>15</sup>These samples were kindly provided by F. Dolezalek and J. Mort.

<sup>16</sup>A. T. Ward, *J. Phys. Chem.* **72**, 744 (1968).

<sup>17</sup>A. Anderson and Y. T. Loh, *Can. J. Chem.* **47**, 879 (1969).

<sup>18</sup>Negative pressure coefficients for internal-mode eigenfrequencies have also been observed in pressure-Raman experiments on the related chain-structure chalcogen crystals Se and Te: W. Richter, J. B. Renucci, and M. Cardona, *Phys. Status Solidi B* **56**, 223 (1973).

While in the present paper these modes in orpiment will not be discussed further, the very fact of intramolecular vibrations which perversely respond to crystal compression by decreasing in frequency reflects the irrelevance of intramolecular forces with respect to the forces which hold together molecular crystals.

<sup>19</sup>R. J. Kobliska and S. A. Solin, *Phys. Rev. B* **8**, 756 (1973).

<sup>20</sup>This is sometimes called the separation approximation. A clear discussion of the degree of validity of this approximation has been given by G. S. Pawley and S. J. Cyvin, *J. Chem. Phys.* **52**, 4073 (1970).

<sup>21</sup>E. A. Wood, *Bell System Tech. J.* **43**, 541 (1964).

<sup>22</sup>R. Zallen, in *Proceedings of the Enrico Fermi Summer School on Lattice Dynamics and Intermolecular Forces, Varenna, 1972*, edited by S. Califano (Academic, New York, 1973).

- <sup>23</sup>J. C. Slater, *Introduction to Chemical Physics* (McGraw-Hill, New York 1939), pp. 217–221.
- <sup>24</sup>E. Grüneisen, *Handbuch der Physik* (Springer-Verlag, Berlin, 1926), Vol. 10, p. 1.
- <sup>25</sup>Our statements about mode-Grüneisen parameters refer, throughout this paper, to zone-center optical phonons. Though  $\gamma_i$  is close to 1 for the Raman mode in Ge, it is smaller for acoustic phonons in this crystal and actually goes negative for some shear-type transverse acoustic phonons near the zone boundary. These negative- $\gamma_i$  modes, though a tiny minority of the crystal eigenvibrations, dominate the phonon population at low temperatures where they give rise to negative thermal expansion. A. Bienenstock, *Philos. Mag.* 9, 755 (1964); R. T. Payne, *Phys. Rev. Lett.* 13, 53 (1964); G. Dolling and R. A. Cowley, *Proc. Phys. Soc. Lond.* 88, 463 (1966).
- <sup>26</sup>S. S. Mitra, C. Postmus, and J. R. Ferraro, *Phys. Rev. Lett.* 18, 455 (1967); C. Postmus, J. R. Ferraro, and S. S. Mitra, *Phys. Rev.* 174, 983 (1968).
- <sup>27</sup>Reference 14, p. 162.
- <sup>28</sup>This is the compressibility of amorphous  $\text{As}_2\text{S}_3$  (the value for crystalline  $\text{As}_2\text{S}_3$ , presently unavailable, should be similar) as reported by F. W. Glaze, D. H. Blackburn, J. S. Osmalov, D. Hubbard, and M. H. Black, *J. Natl. Bur. Stand.* 59, 83 (1957).
- <sup>29</sup>The equivalent of Eq. (7) appears, in two different derivations, in the comprehensive treatment by Cerdeira *et al.* (Ref. 5) of stress-induced shifts in the diamond structure.
- <sup>30</sup>S. Ganesan, A. A. Maradudin, and J. Oitmaa, *Ann. Phys. (N.Y.)* 56, 556 (1970). Certain algebraic errors in this paper are discussed in Ref. 5.